

Investigation on Loss of Tail-rotor Effectiveness of Helicopter with Ducted Fan Tail Rotor

Nahyeon Roh¹, nahyeon7782@pusan.ac.kr, *Pusan National University, Busan, South Korea*

Donghun Park², parkdh@pusan.ac.kr, *Pusan National University, Busan, South Korea*

Sejong Oh³, tazo@pusan.ac.kr, *Pusan National University, Busan, South Korea*

Abstract

The loss of tail rotor effectiveness(LTE) means steep loss of yawing stability in particular flight condition due to the reduction of tail rotor performance. In this study, numerical analysis is conducted to investigate the LTE characteristics of the ducted fan tail rotor. The complete helicopter configuration(main rotor, ducted fan tail rotor, fuselage, and empennage) is simulated to obtain the mechanism of wake interaction for a range of whole crosswind angle, from 0° to 360° . It is confirmed that both the main rotor wake and port wing wake are immersed within tail rotor disk by the suction force of tail rotor. The main rotor wake rotates in the opposite direction to the tail rotor, and it contributes to the improvement of thrust. The port wing wake works oppositely. As the flow entered from the front side, both magnitude and vibration of thrust are increased due to the broad influence of the main rotor wake. Nevertheless, direct impingement of wakes is prohibited by the structures of tail rotor system, and also substantial wake of tail rotor prevents re-entering of tip vortex. Consequently, the ducted fan tail rotor maintains acceptable thrust variation in comparison with the open type tail rotor.

1. Symbols and abbreviations

1.1. Symbols

D_{MR}	Diameter of main rotor	[m]
r_{TR}	Radius of tail rotor	[m]
y^+	Nondimensional wall distance	[-]
ψ_{MR}	Azimuth angle of main rotor	[deg]
ψ_{TR}	Azimuth angle of tail rotor	[deg]
T	Thrust	[kg · m/s ²]
C_T	Thrust coefficient	[-]
P	Power	[kg · m ² /s ³]
M	Moment	[kg · m ² /s ²]

1.2. abbreviations

LTE	Loss of Tail-rotor Effectiveness
VRS	Vortex Ring State
ADM	Actuator Disk Method
IASM	Improved Actuator Surface Method
TA	Top-After

2. INTRODUCTION

2.1. Loss of Tail-rotor Effectiveness (LTE)

The helicopter operates in a highly complex and unsteady flow-field due to the substantial interference between components. This interaction can affect the performance, stability, and handling qualities of the helicopter. Notably, the performance of the tail rotor is considerably influenced by the freestream and wake generated by fuselage or main rotor. It affects the lateral stability of the helicopter.

National transportation safety board(NTSB) defined the loss of tail rotor effectiveness as LTE[1]. The LTE means loss of yawing stability results from the loss of tail rotor performance. NTSB suggested three primary hazard zones according to the direction and speed of crosswind. Three reasons are divided as follows(Fig. 1): 1) Disk vortex interference: increase of tail rotor thrust oscillation due to the direct impingement of the main rotor wake. 2) Vortex ring state(VRS): decrease in magnitude and increase in oscillation of tail rotor thrust by re-entering tip vortex. 3) Weathercock stability: embarrassing yawing moment caused by rotational force in the freestream direction.

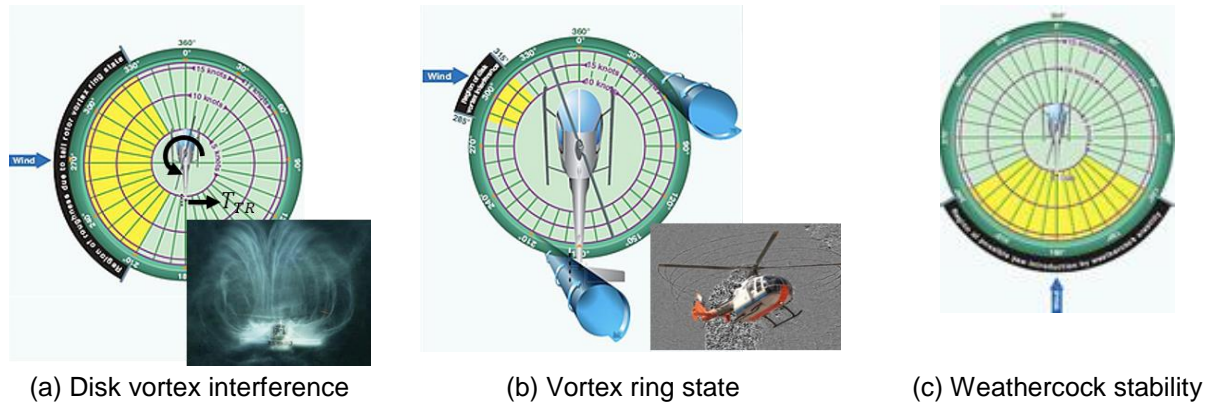


Figure 1. Loss of tail rotor effectiveness contour

2.2. Previous Study

Conventional Tail Rotor

To comprehend the aerodynamic characteristics of open type tail rotor with crosswind, many studies have been investigated both theoretically and experimentally. Robert et al.[2, 3] conducted experimental study about the tail rotor performance in rearward flight, under in ground effect. Ellin et al.[4] performed flights test using a Lynx helicopter and divided flight envelope into six regions, with a different mechanism of main rotor/tail rotor interaction. Timothy et al.[5,6] analyzed the aerodynamic effect by the sense of rotation of the tail rotor and crosswind direction. He confirmed that the tail rotor which is operated at a pretransitional advance ratio shows aperiodic meandering over a time scale that is significantly longer than the period of main rotor revolution.

Ducted Fan Tail Rotor

Since 1968, Aerospatiale has developed the ducted fan tail rotor(Fenestron®) as an alternate solution to the conventional tail rotor for light helicopters[7, 8]. This tail rotor system including fixed(shroud, outer shroud, hub, vertical fin) and rotating(rotor) parts, has the advantage of preventing safety accidents caused by high speed rotating rotor as well as external impact.

By the previous studies, flow and aerodynamic characteristics of the ducted fan in hover flight are well defined[9-12]. On the contrary, the investigations in crosswind were relatively less. Rajagopalan et al. [13] conducted a numerical study about thrust changes in the left/right sideward flight condition. Emre[14] analyzed the flow field and performance of RAH-66 in hover

and sideward flight and presented the variations of the yawing moment.

However, since the most of the previous study did not perform the unsteady analysis about full configuration, it is hard to suggest the interaction effect between components. Also, performance on variable crosswind direction was not well understood.

2.3. Research Objectives

In this study, the LTE characteristics of a helicopter with ducted fan tail rotor are investigated. Numerical analysis has been carried out for complete helicopter configuration(main

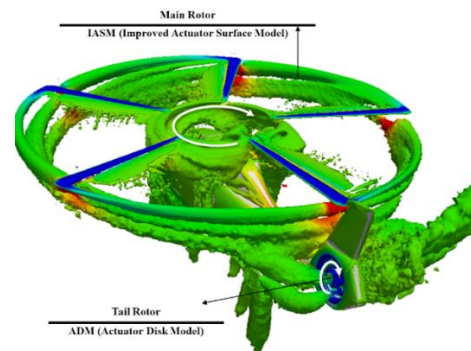


Figure 2 Analysis configuration and rotor model method



Figure 3 Eurocopter EC155b1[18]

rotor, ducted fan tail rotor, fuselage, and empennage).

The goals of this study are as follows: 1) Suggestion the flow-field characteristics of ducted fan tail rotor due to the interactions between the main rotor/tail rotor/body by simulating the complete helicopter configuration, 2) Evaluation the averaged forces, fluctuation of aerodynamic forces and yawing moment according to crosswind directions, 3) Comparison of the LTE characteristics between conventional open type tail rotor and ducted fan tail rotor.

3. NUMERICAL METHOD

3.1. Numerical Procedures

The improved actuator surface method(IASM)[15] and actuator disk method(ADM)[16] is applied to simulate the main rotor and tail rotor, respectively. The actuator surface method is proper for analyzing main rotor performance since it can simulate the unsteady motion of the blades with tip vortex strength and vortex trajectory. Meanwhile, even the actuator disk method simulates the time-averaged flow of the rotor disk, it is suitable to analyze the ducted fan tail rotor. These two methods coupled with numerical solver improve computational efficiency significantly. Fig. 2 shows the investigated configuration with rotor modeling methods.

The IASM and ADM are adapted to open source code, OpenFOAM[17]. 2nd order backward

scheme for time integration and 2nd order Gauss linear upwind scheme for convective terms are used with $\kappa - \omega$ SST turbulence model.

3.2. Analysis Configuration & Condition

The analysis configuration is similar to Eurocopter EC 155b1(Fig. 3). Every part except fuselage are same with the EC 155b1, part the fuselage is simplified.

The principal parameters for the main and tail rotors are given in Table1 and Table2, respectively. The main rotor rotates in clockwise when viewed from above, hence the tail rotor

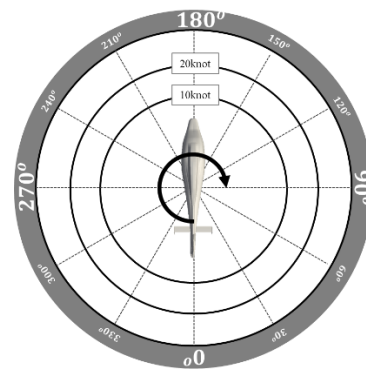
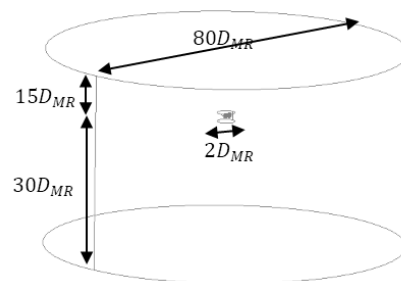
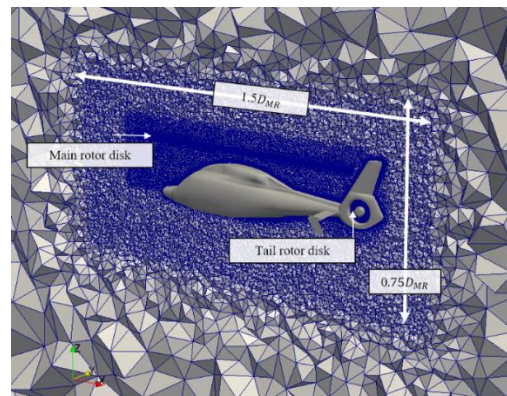


Figure 4 Analyzed flight condition



(a) Topology of analyzed domain



(b) Grid clustering around helicopter

Figure 5 Computational domain

Table 1. Main rotor data

No. of blades	5
No. of airfoil	3 (OAF2XX Series)
Rotor radius	6.301 m
Rotational Speed	342 rpm

Table 2. Tail rotor data

No. of blades	10
No. of airfoil	5 (OAF3XX Series)
Rotor radius	0.546 m
Rotational Speed	3579 rpm

produces a force to port in trimmed flight. The tail rotor rotates in Top-After(TA) direction(Fig. 2), implying that its blades travel rearward at the top of the disk. All blades are assumed to be rigid. Collective pitch angles of the main rotor and tail rotor are set to hover flight condition. The thrust of main rotor has a less than 0.5% error to MTOGW, including body forces induced by main rotor. Also, thrust of tail rotor compensates the torque of the whole configuration within 2.5% error to main rotor torque.

Performance changes due to the crosswind acting on a helicopter in hover flight are analyzed. The flight conditions are chosen based on the LTE region suggested by the previous study on the open type tail rotor. With 20knot of wind speed, crosswind angle is changed from 0° to 360° with 30° interval(Fig. 4).

3.3. Computational Domain

The computational domain included a helicopter with ducted fan tail rotor. A cylinder topology was used for the grid geometry by considering the various freestream direction. As shown in Fig. 5a., the cylinder encompasses the region of $-20 \leq x/D_{MR} \leq 20$, $-20 \leq y/D_{MR} \leq 20$, $-30 \leq z/D_{MR} \leq$

15, and the computational grid consisted of 19 million cells. To accurately resolve the flow around tail rotor, generate a more clustered mesh in the vicinity of the helicopter(Fig. 5b). A wall function is applied for the sub-layer. Therefore, a viscous grid spacing of 6×10^{-3} was specified on the wing surface with the aim of setting $y^+ \cong 30$.

4. Results

The results presented in this paper are extracted after enough simulation till both rotors obtain periodicity. Presented contours and iso-volume are snapshots at $\psi_{MR} = 0^\circ$ in the last revolution. The aerodynamic forces are calculated by using the data in the last main rotor revolution. In case of results appear to be very little periodicity, data in last 3-revolutions are used. The tail rotor only operates condition, without main rotor, is named as "TR Only". For convenience, each flight condition along the crosswind angle are designated by the angle(e.g. 0° , 180°)

4.1. Flow Characteristics

Wake Interactions

The crosswind direction affects to the interaction between the main rotor-tail rotor/main rotor-

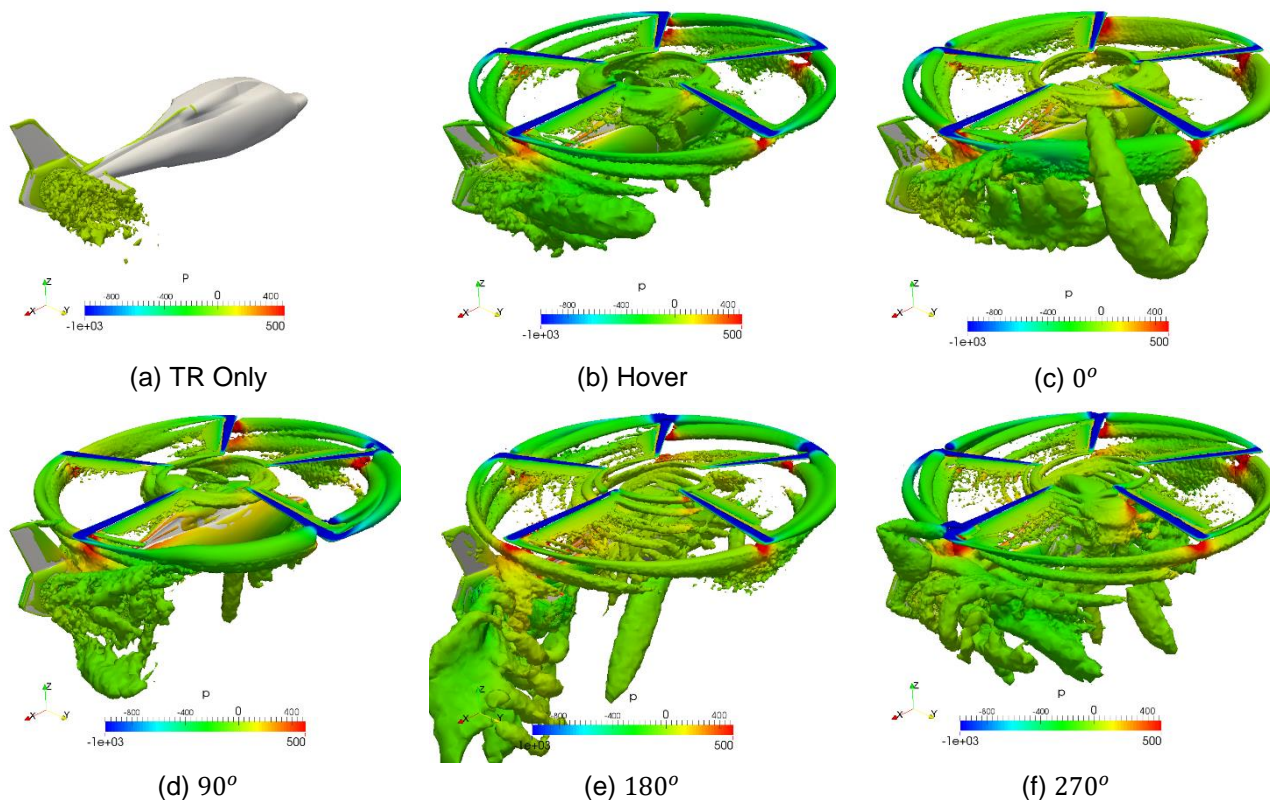


Figure 6 Q iso-volume colored with pressure along sideward direction

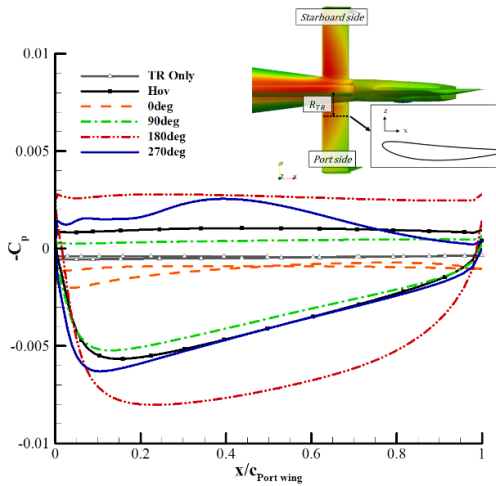


Figure 7 Pressure distribution on port wing at $y/R_{TR} = 1$

fuselage, as well as wake direction of each rotor. To confirm the effect of crosswind on the wake interactions, compare the iso-volume of each flight condition (Fig. 6) with 90° interval. Also, to clarify the influence of main rotor, compare with only tail rotor operating case (Fig. 6a, TR Only case). Through fig. 6., it can be seen that the main rotor always induces complicated flow around the tail rotor. The wake of the isolated tail rotor (Fig. 6a) solely extends some distance, whereas another case quite strongly dependent on main rotor. When the flow entered from 0° (Fig. 6c), tail rotor wake is bent toward main rotor and affects to main rotor wake. The effect of main rotor to tail rotor is most pronounced in 180° (Fig. 6e). At this condition, wake of tail rotor moves toward down due to the downwash of main rotor. Simultaneously, spiral geometry is formed because of the periodicity of main rotor. The wake interaction in 90° and 270° are relatively less since these sideward flow are aligned to tail rotor wake direction.

Effect on Port Wing

The port wing is a rectangular wing with a reverse-camber airfoil. The wake generated by port wing is suctioned by tail rotor and it brings out loss of tail rotor performance.

Figure 7., which indicates the pressure distribution on port wing at $y/R_{TR} = -1$., reveals that the crosswind angle directly affects the pressure distribution on port wing. In TR Only case, pressure difference are nearly zero. The effect of main rotor in 0° is also insignificant. On the other hand, the pressure difference is distinct at 180° where the influence of the main rotor is clearly illustrated from Fig. 7. The increase of lift caused by pressure difference leads to strong vortex.

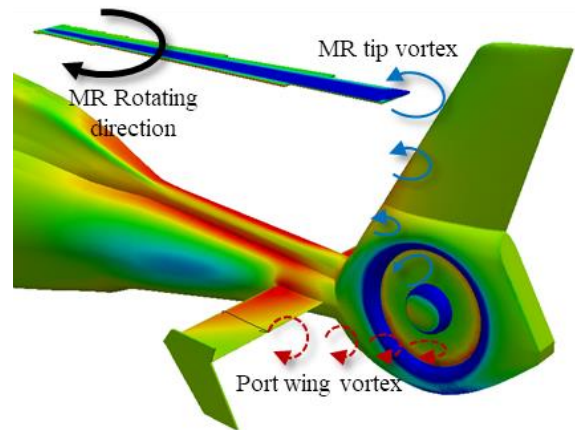


Figure 8 Schematic of wake directions on tail rotor

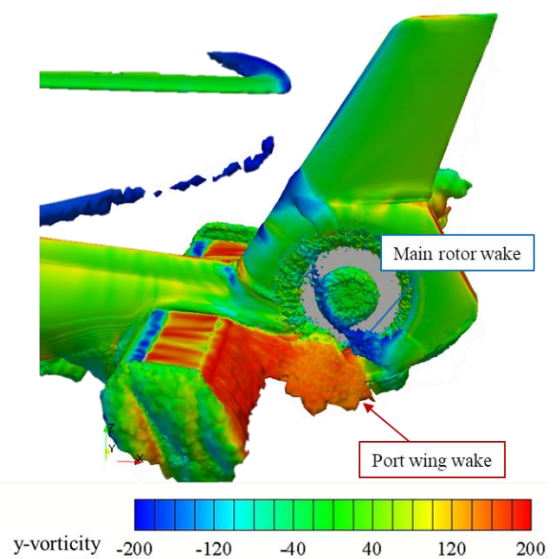


Figure 9 Iso-volume of vorticity magnitude colored with y-vorticity in 180°

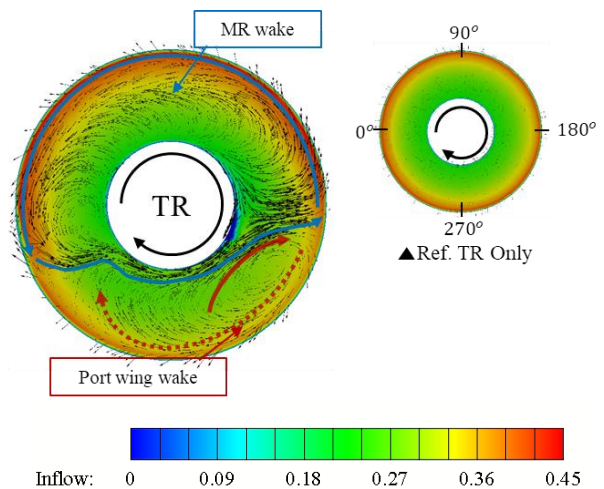


Figure 10 Inflow and velocity vector in hover flight

Thus, it can be expected that the strong port wing wake will occur as the freestream entered from front side.

Tail Rotor Disk Flow

Both the main rotor wake and port wing wake are complexly immersed within tail rotor disk. Fig. 8 is the schematic of how the main rotor wake and port wing wake applied to the tail rotor. Fig. 9 shows iso-volume of vorticity magnitude colored with y-vorticity (negative in tail rotor rotating direction) in 180° . Through Fig. 8 and Fig. 9, it is confirmed that the main rotor wake and port wing wake are crucial to the tail rotor, and two wakes are rotated in opposite directions. The main rotor wake rotates in a counter-clockwise direction, opposite to the tail rotor. The port wing wake has the same sense of rotation as the tail rotor. Both wakes are not impinged directly into the tail rotor disk, but are entered by the suction force of the tail rotor. It is more clearly seen by the port wing wake. The port wing wake that initially moves downward is re-sucked by the tail rotor, and it affects the bottom region of the tail rotor disk. The outboard of the port wing wake, not affected by the tail rotor suction force, flows downward along the main rotor downwash direction.

Figure 10, inflow contour with velocity vector in hover flight, represents the influence of the main rotor and port wing wake on the tail rotor disk. To clarify the effect of the wakes, TR Only is compared. The azimuth angle of the tail rotor is also plotted. The solid arrow marked over the velocity vector means the

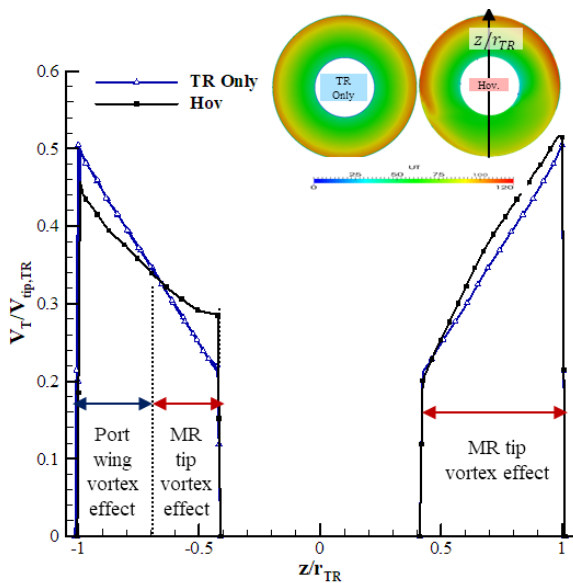


Figure 11 Tangential velocity in hover flight

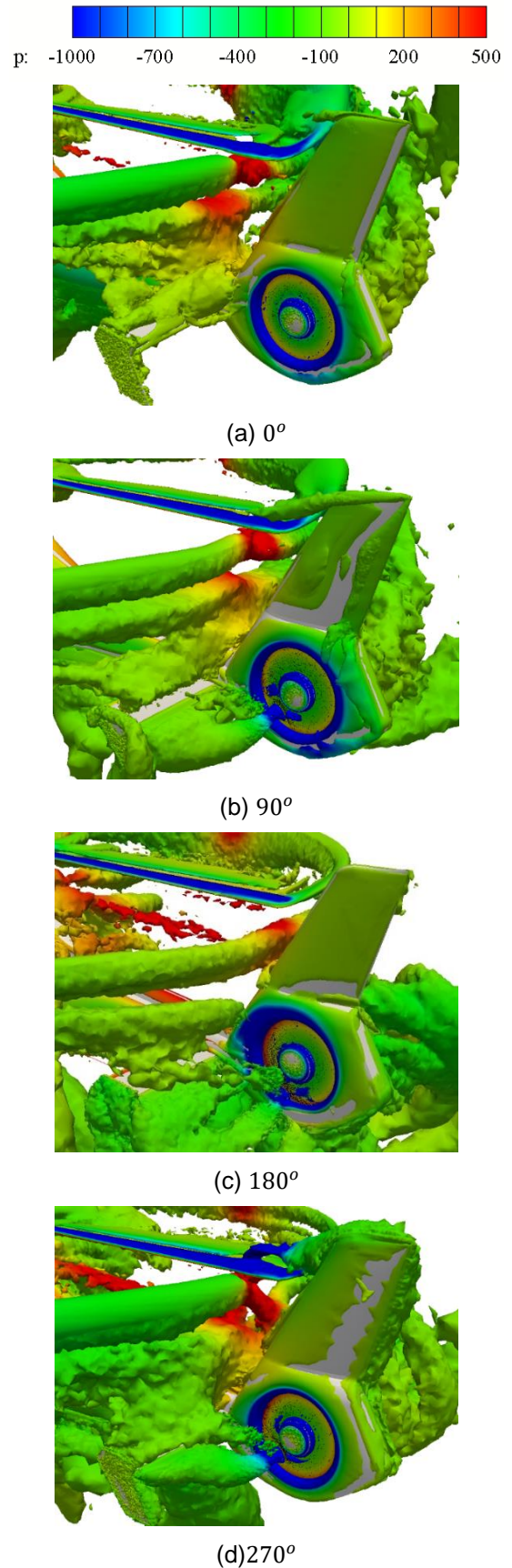


Figure 12 Q iso-volume colored by pressure

opposite direction to tail rotor rotation, and the dotted arrow means the same direction. In hover flight, the main rotor wake cover the entire upper side($\psi_{TR} = 0^\circ \sim 180^\circ$) and just below of the hb. Thereby, the velocity that rotates in the opposite direction of tail rotor(soild arrow) is induced at the grater part of tail rotor disk. The center of port wing wake is located nearby $\psi_{TR} = 210^\circ$, it affects the most area of lower part. The wake rotates in the same direction with tail rotor at the tip(dotted arrow) and has opposite direction around the hub(solid arrow).

The additional velocity induced by wake brings about the change in relative velocity. And the faster relative velocity leads to the faster tangential velocity. Fig. 11, which indicates opposite direction to tail rotor rotation, and the dotted arrow means the same direction. In hover

flight, the main rotor wake cover the entire upper side($\psi_{TR} = 0^\circ \sim 180^\circ$) and just below of the hub. Thereby, the velocity that rotates in the opposite direction of tail rotor(soild arrow) is induced at the greater part of tail rotor disk. The center of port wing wake is located nearby $\psi_{TR} = 210^\circ$, it affects the most area of lower part. The wake rotates in the same direction with tail rotor at the tip(dotted arrow) and has opposite direction around the hub(solid arrow).

tangential velocity at vertical slice of tail rotor disk, demonstrates the change of relative velocity by two wakes. As can be seen in the graph, tangential velocity in most of upper side($z/r_{TR} > 0.4$) is increased result from effect of main rotor wake. Whereas at lower tip side($z/r_{TR} < -0.7$), tangential velocity is decreased due to the port wing wake.

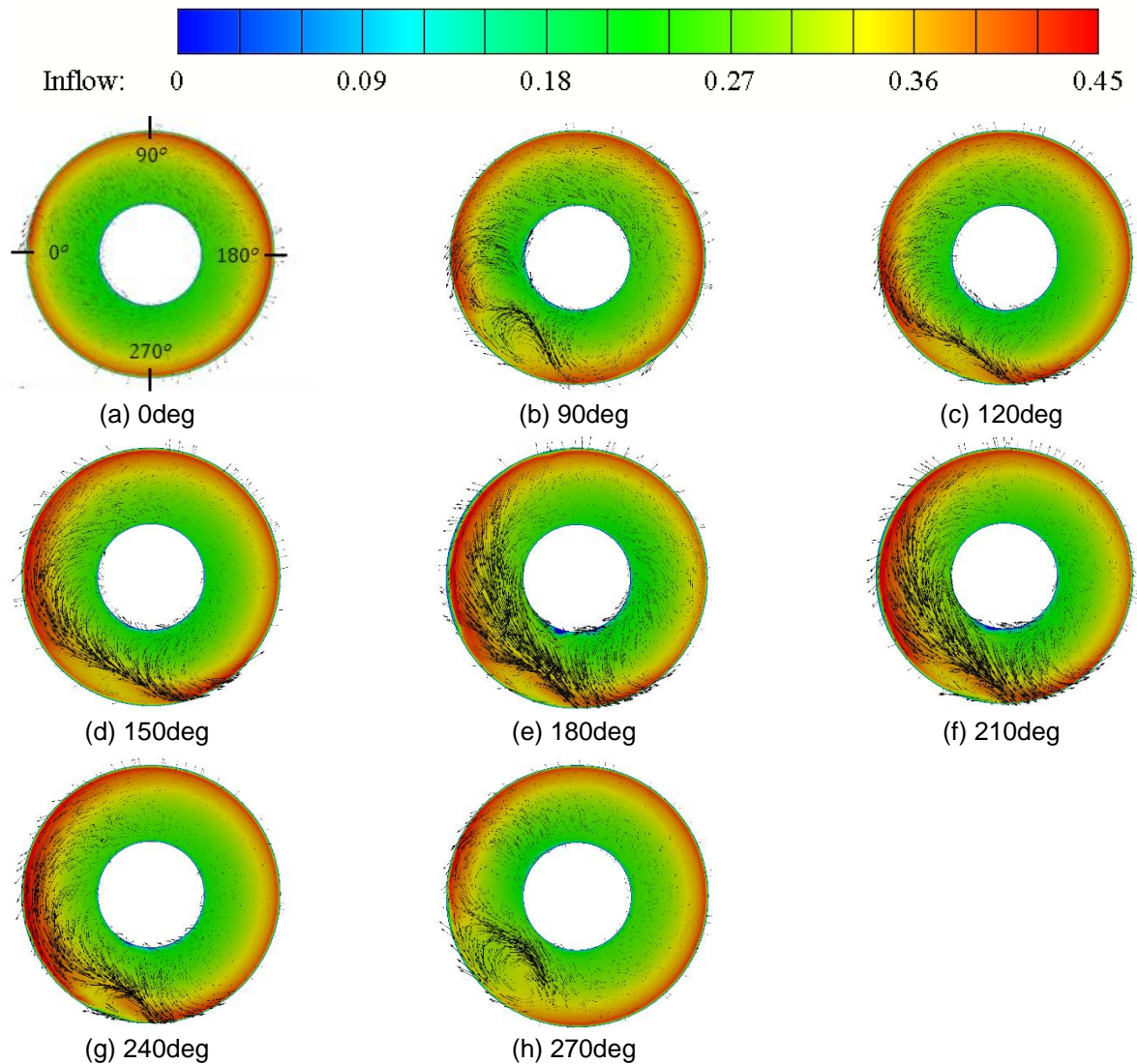


Figure 13 Inflow contour with velocity vector along the crosswind angle

Increasing the tangential velocity derives a decrease in induced angle of attack and increase in effective angle of attack. Therefore, it could be expected that the main rotor wake results in thrust improvement. The expectation confirmed by the inflow contour, which shows apparent increase at the tip region. That is, thrust of tail rotor rotates in TA direction is improved by interacting with the main rotor wake. It is the reason why most of tail rotor (regardless open type or ducted fan tail rotor) take the TA sense of rotation.

The effect of crosswind on tail rotor disk flow is analyzed. Fig. 12 represent iso-volume of Q-criterion around tail rotor system with 90° Interval. Fig. 13 shows a series of inflow contour (0° and 90°~270° with 30° interval) with velocity vector induced by the main rotor and port wing wake. As confirmed before, when the flow entered from rearward side, the main rotor wake rarely impinge on tail rotor disk since the wake moves toward forward. Meanwhile, as the flow entered from front side, the center of main rotor wake moves toward hub. Therefore it affects more broad range of tail rotor disk. In 180°, the main rotor wake covers the broadest range, where the most area of left side ($\psi_{TR} = 270^\circ \sim 90^\circ$). Indeed through the comparison between Fig.13d and Fig.13f, which are bias 30° respectively with nose as the center, it is confirmed that the main rotor appears more stronger effect when the freestream entered from a tail rotor inlet direction.

Since the port wing wake is influenced by main rotor wake (Fig. 7), the strength and range of port wing wake show similar trends to main rotor wake. As the port wing wake crossing the tail boom instead of entering the tail rotor disk, vector generated by both wakes in 0° is nearly zero. In contrast, when inflow comes from upstream, the port wing wake has local influences on bottom part of tail rotor disk. In case of sideward flow, relatively weak wake influences broad area.

Through the analysis on flow characteristics, the distinct advantages of ducted fan tail rotor than conventional open type tail rotor are obtained. For the conventional open type tail rotor, the wakes directly impinge on rotor disk cause it is exposed to outside. On the other hand, the ducted fan tail rotor which is shrouded by fixed parts of tail rotor system (shroud, outer shroud, vertical fin) is protected from external effect, and thus most of the wakes are bumped on fixed parts. Only the

main rotor and port wing wake are re-sucked by suction force generated by tail rotor thrust.

4.2. Aerodynamic Forces

Averaged Forces

Figure 14 compares the averaged thrust/power of both rotors along the crosswind angle. The changes in aerodynamic characteristics to the hover flight are defined as Eqs. (1) – (2).

$$(1) \quad \Delta T(\%) = \frac{T - T_{Hover\ flight}}{T_{Hover\ flight}} \times 100$$

$$(2) \quad \Delta P(\%) = \frac{P - P_{Hover\ flight}}{P_{Hover\ flight}} \times 100$$

As shown in Fig. 14a., the thrust of both main rotor and tail rotor are increased as flow entered from front side. In the forward flight, the tail rotor is located downstream of the main rotor. Therefore the tail rotor wake rarely entrained into main rotor. Because the less interference effect on main rotor offers isolated rotor-like behavior, the ΔT of main rotor is increased due to the reduction of additional 3-D effect.

In contrast, for the tail rotor, operating as an isolated rotor does not always means enhancement of performance. The aerodynamic performance of tail rotor is decided by relation between the main rotor, which induces thrust improvement, and port wing wake, which bring out loss of thrust. For example, as the flow entered from forwarding direction, results below arise at the same time; 1) Increase in the strength of main rotor wake, 2) Expansion of the range of main rotor wake, 3) Inducing stronger port wing wake result from stronger main rotor wake, 4) Shrinkage the range of port wing wake by the influence of main rotor downwash. As a result, the tail rotor thrust changes from -13% for the 330° where the adverse effect of the port wing wake is dominant, upto 7.5% for 180° where the main rotor wake covers the largest range.

To obtain directional stability characteristics of the helicopter, variation of yawing moment along with crosswind angle is compared (Fig. 14c). The changes in yawing moment to hover flight is defined as Eqs. (3). The yawing moment is computed with respect to the center of main rotor.

$$(3) \quad \Delta M_z(\%) = \frac{M_z - M_{z,Hover\ flight}}{M_{z,Hover\ flight}} \times 100$$

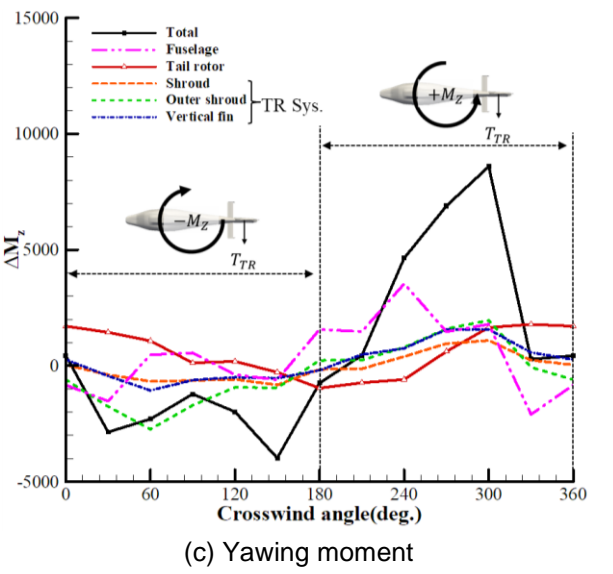
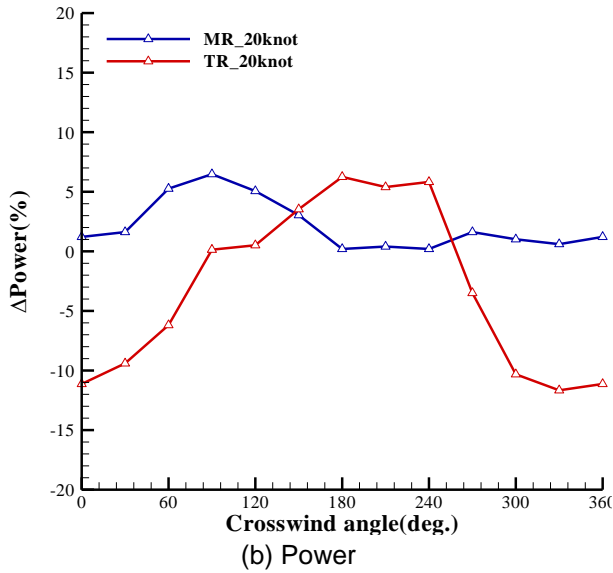
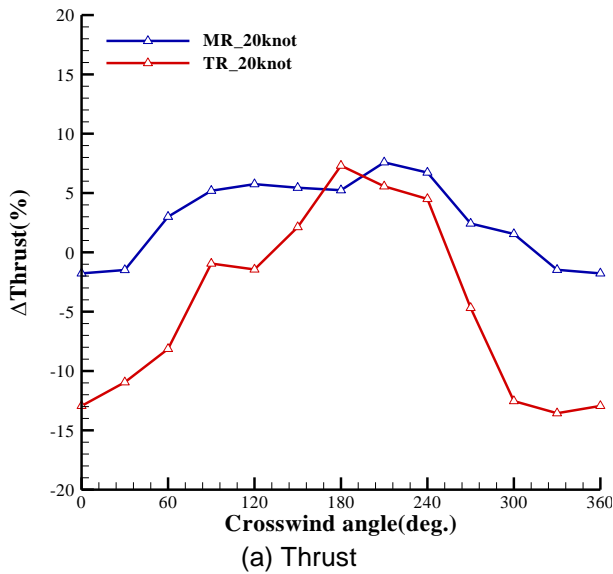


Figure 14 Averaged aerodynamic forces of tail rotor

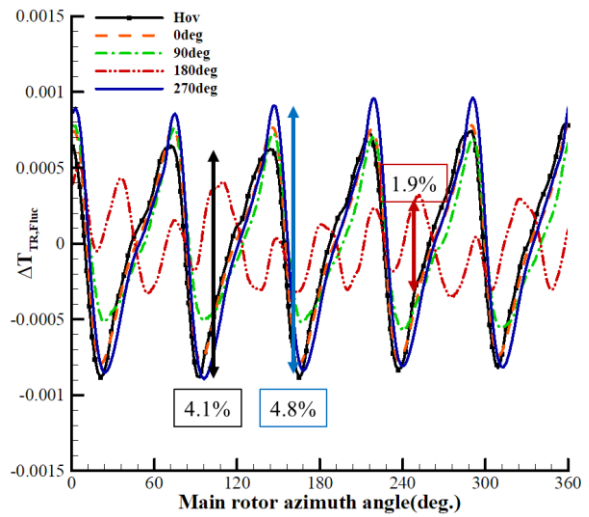


Figure 15 Fluctuation of tail rotor thrust during one revolution of main rotor

The shroud, outer shroud, and vertical fin are exposed to freestream. Therefore these are respectively independent on the main rotor wake. As a result, the moment of tail rotor system shows expected trend along the crosswind angle. In contrast, the fuselage, which undergoes a main rotor effect, shows a non-constant trend. The anti-torque force generated by tail rotor is changed by the variation of tail rotor thrust, as presented in Fig. 14a.

The total yawing moment is in the opposite direction to the movement of the tail rotor, in right crosswind condition (180°~360°). Especially in 300°, the significantly strong yawing moment is induced over 8000Nm, which is about 33% of main rotor torque in hover flight.

Force Fluctuation

Not only the averaged force but also fluctuation of thrust is associated with stability and controllability of helicopter. The fluctuation of tail rotor thrust coefficient to the averaged value at each flight condition, $\Delta C_{T,TR,Fluc}$, is defined as Eq. (4).

$$(4) \quad \Delta C_{T,TR,Fluc}(\%) = \frac{C_{T,TR} - C_{T,TR,average}}{C_{T,TR,average}} \times 100$$

Figure 15 shows the results during the one revolution of main rotor. In all cases except the 180°, shape and amplitude are similar to hover flight. Among these, the amplitude to averaged force is varied from 4.09% for hover upto 4.5% for 270°. The 180° indicates the minimum amplitude for 1.9%, whereas impair periodicity. This is

interpreted as a result of the strong impingement of main rotor and port wing wake, as suggested previous sub-section of this paper. And also, unsteadiness on tail rotor thrust in 180° suggested in this paper has consistency with results of the previous study[5], that the tail rotor wake exhibits aperiodic meandering in specific flight condition.

4.3. Loss of Tail-rotor Effectiveness

The ducted fan tail rotor shows acceptable thrust variation than open type tail rotor. It is consequence of the inherent advantage for ducted fan tail rotor; 1)the rotor is protected by the tail rotor system, such as shroud, outer shroud, and vertical fin, 2)rotor wake is expanded along the diffuser with strong intensity. The structures protect the direct impingement of the main rotor wake and port wing wake. Moreover, the substantial wake keeps disturbing the wake entering through the bottom surface of shroud.

As a consequence, the ducted fan could restrain the steep reduction or severe vibration of thrust in the disk vortex interference region($120^\circ \sim 150^\circ$, Fig. 1a) and VRS region($30^\circ \sim 150^\circ$, Fig. 1b) of the conventional tail rotor, since the re-entering of tip vortex and direct invasion of main rotor wake through diffuser is prevented. Therefore, despite the thrust of open type tail rotor is decreased maximum 80%[19], thrust of ducted fan is reduced about 13% with 0° . Also, fluctuation of thrust to averaged value is about 4.5%, even the that of open type tail rotor is over the 50%[20].

The yawing moment is increased about 33% of main rotor torque at 300° . It reveals that the helicopter tends to rotate in main rotor rotating direction and undesirable yawing moment will be occur. Nevertheless, due to the lack of data about the available tail rotor collective pitch angle, quantitative analysis about weathercock stability region($300^\circ \sim 60^\circ$ Fig 1c) are could not concluded.

5. Conclusion

In an effort to investigate the LTE characteristics of ducted fan tail rotor, numerical analysis has been carried out on the helicopter that has a ducted fan tail rotor. This study suggests results of interference effect between each component of a helicopter. Furthermore, TR Only case is simulated to comprehend the difference in the

wake interference mechanism by the presence of a main rotor. Consequently, the following conclusions are reached;

1) The main rotor wake adds periodic wake structure to tail rotor wake. The influence on the tail rotor is reduced in the rearward flight condition, whereas it increased in forward flight condition.

2) Both the main rotor and port wing wakes are immersed within the tail rotor disk. The main rotor wake rotates in the opposite direction to tail rotor, and it contributes to increasing of tangential velocity, that is an improvement of thrust. The port wing wake works oppositely. As a result, the tail rotor thrust changes from 7.5% for 180° upto - 13% for the 330° .

3) The ducted fan tail rotor could maintain controllability in disk vortex interference region and VRS region of conventional open type tail rotor. The structures of tail rotor system protect the direct impingement of the wakes through lower/upper surface of the shroud. Moreover, substantial wake of tail rotor prevents the re-entering of tip vortex.

4) It is confirmed that the helicopter tends to rotate in the opposite direction to the movement of the tail rotor, in right crosswind condition. Nevertheless, further studies with enough data are needed to quantitatively estimate the weathercock stability characteristics.

5. Reference

- [1] WHITE, W. J. Unanticipated right yaw in helicopters. Advisory Circular, 1995, 90-95.
- [2] Huston, R. J., & Morris Jr, C. E. (1971). A wind tunnel investigation of helicopter directional control in rearward flight in ground effect.
- [3] Huston, R. J., & Morris, C. E. (1970). A Note on a Phenomenon Affecting Helicopter Directional Control in Rearward Flight. *Journal of the American Helicopter Society*, 15(4), 38-45.
- [4] Ellin, A. D. S. (1993). An Inflight Investigation of LYNX AH MK5 Main Rotor/Tail Rotor Interactions. European Rotorcraft Forum, (Vol. 19, pp. C6-C6)
- [5] Fletcher, T. M., & Brown, R. E. (2008). Main Rotor-Tail Rotor Interaction and Its Implications for Helicopter Directional Control. *Journal of the American Helicopter Society*, 53(2), 125-138.
- [6] Fletcher, T. M., & Brown, R. E. (2010).

Helicopter tail rotor thrust and main rotor wake coupling in crosswind flight. *Journal of aircraft*, 47(6), 2136-2148.

[7] Mouille, R. (1970). The "Fenestron," Shrouded Tail Rotor of the SA. 341 Gazelle. *Journal of the American Helicopter Society*, 15(4), 31-37.

[8] Vuillet, A., & Morelli, F. (1986). New aerodynamic design of the Fenestron for improved performance.

[9] BOURTSEV, B. (2000). Fan-in-Fin Performance at Hover Computational Method. In *Proc. 26th European Rotorcraft Forum, 2000*.

[10] J.K. Lee, O. J. Kwon & J. M. Kim. (2000). Rotor-Fuselage Interactional Aerodynamic Analysis Using Unstructured Meshes, *Journal of the Korean Society for Aeronautical & Space Sciences*, 28(1), 36-45

[11] Cao, Y., & Yu, Z. (2005). Numerical simulation of turbulent flow around helicopter ducted tail rotor. *Aerospace Science and Technology*, 9(4), 300-306.

[12] Mouterde, E., Sudre, L., Dequin, A. M., D'Alascio, A., & Haldenwang, P. (2007). Aerodynamic computations of isolated Fenestron® in hover conditions.

[13] Rajagopalan, R. G., & Keys, C. N. (1997). Detailed Aerodynamic Analysis of the RAH-66 FANTAIL™ Using CFD. *Journal of the American Helicopter Society*, 42(4), 310-320.

[14] Alpman, E., Long, L. N., & Kothmann, B. D. (2004). Understanding Ducted Rotor Antitorque and Directional Control Characteristics Part I: Steady State Simulation. *Journal of Aircraft*, 41(5), 1042-1053.

[15] T. W. Kim, S. J. Oh, K. & J. Yee., The Extension and Validation of OpenFOAM Algorithm for Rotor Inflow Analysis using Actuator Disk Model. *Journal of The Korean Society for Aeronautical and Space Sciences*, Vol. 39, No. 12, 1087~1096.

[16] T. W. Kim, S. J. Oh, K. & J. Yee., Improved actuator surface method for wind turbine application. *Renewable Energy*, 2015,16-26.

[17] www.openfoam.com

[18] <https://www.airbus.com/>

[19] Leishman, G. J. (2006). *Principles of helicopter aerodynamics with CD extra*. Cambridge university press.

[20] Yaggy, P. F., & Mort, K. W. (1963). *Wind-tunnel tests of two vtol propellers in descent*. National Aeronautics and Space Administration.